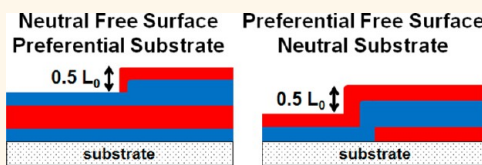


# Consequences of Surface Neutralization in Diblock Copolymer Thin Films

Sangwon Kim,<sup>†,⊥</sup> Christopher M. Bates,<sup>‡,⊥</sup> Anthony Thio,<sup>§</sup> Julia D. Cushen,<sup>§</sup> Christopher J. Ellison,<sup>§</sup> C. Grant Willson,<sup>‡,§,\*</sup> and Frank S. Bates<sup>†,\*</sup>

<sup>†</sup>Department of Chemical Engineering and Materials Science, University of Minnesota, Minneapolis, Minnesota 55455, United States and <sup>‡</sup>Department of Chemistry and <sup>§</sup>McKetta Department of Chemical Engineering, The University of Texas at Austin, Austin, Texas 78712, United States. <sup>⊥</sup>These authors contributed equally.

**ABSTRACT** Two high- $\chi$  block copolymers, lamella-forming poly(styrene-*block*-[isoprene-random-epoxysoprene]) (PS-PEI78, with 78 mol % epoxidation) and lamella-forming poly(4-trimethylsilylstyrene-*block*-D,L-lactide) (PTMSS-PLA), were used to study three combinations of interfacial neutrality involving at least one neutral interface. PS-PEI78 annealed on a nonpreferential polymer mat (SMG) produced perpendicular



lamellae independent of film thickness, indicating a neutral substrate and neutral free surface. In contrast, the presence of only one neutral interface results in the formation of surface topography ("islands" and "holes") with  $0.5L_0$  step heights. PS-PEI78 (neutral free surface) annealed on PS brush (PS block preferential) forms "half" islands and holes. The inverse experiment, PTMSS-PLA (with a PTMSS preferential free surface) annealed on a neutral (or near neutral) substrate surface, also generates  $0.5L_0$  topography. These "half" island and hole structures are stable to extended thermal annealing. PS-PEI78 exposes both blocks at the free surface in contrast to PTMSS-PLA, which exposes just one. All three combinations of interfacial neutrality are explained by the precise balancing of the wetting tendencies of the two blocks. Evolution of the  $0.5L_0$  motifs appears to be facilitated by a preference to form half-period thick nuclei in the initial stages of morphological development.

**KEYWORDS:** block copolymer · thin film interfaces · thickness quantization · islands · holes ·  $0.5L_0$  · step height

Thin films of block copolymers (BCPs) have potential for applications in a variety of important technologies including membranes<sup>1</sup> and lithographic patterning processes for next-generations of semiconductors<sup>2</sup> and hard disk drives.<sup>3</sup> Most of these thin film applications demand precise control of the BCP morphology and orientation of the structures such that they are perpendicular to the substrate. Only through precise engineering of the BCP materials and interfaces they encounter can this be achieved. Thus, extensive work has gone into understanding the role of interfaces on BCP thin film self-assembly.

Early work dealing with solvent-cast films of poly(styrene-*block*-butadiene) suggested that the underlying morphologies could mimic those found in the bulk.<sup>4,5</sup> Subsequent studies concluded that strong deviations from bulk composition profiles exist at the thin film free (top) surface for a number of block copolymers including poly(styrene-*block*-dimethylsiloxane) (PS-PDMS),<sup>6</sup> poly(styrene-*block*-methyl methacrylate)

(PS-PMMA),<sup>7</sup> and poly(styrene-*block*-ethylene oxide) (PS-PEO).<sup>8</sup> Partial or complete surface segregation of the low surface energy block minimizes the overall interfacial energy at the free surface. However, solvent casting often leads to nonequilibrium structures, as evidenced by the formation of surface topography upon thermal annealing, usually referred to as "terracing" (with, for example, poly(styrene-*block*-butadiene)).<sup>9</sup> Clarification and unambiguous determination of the equilibrium thin film behavior of lamella-forming BCPs was provided by Coulon,<sup>10</sup> Russell,<sup>11</sup> and co-workers based on their insightful work with PS-PMMA.

BCP lamellae orient parallel to the substrate in the presence of preferential interfaces. If the same block wets the substrate and free surfaces (symmetric wetting), the film thickness quantizes to  $nL_0$ , where  $L_0$  is the bulk periodicity and  $n$  is an integer. In contrast, if different blocks wet the substrate and free surfaces (asymmetric wetting), the film thickness quantizes to  $(n + 0.5)L_0$ . After annealing, average as-cast

\* Address correspondence to  
bates001@umn.edu,  
willson@che.utexas.edu.

Received for review July 15, 2013  
and accepted October 16, 2013.

Published online October 16, 2013  
10.1021/nn403616r

© 2013 American Chemical Society

film thicknesses ( $L_{\text{avg}}$ ) that are incommensurate with the preferred wetting condition for a given block copolymer spontaneously produce surface topography referred to as islands and holes.<sup>12,13</sup> The formation of islands or holes is thickness-dependent: for symmetric wetting, islands form when  $nL_0 < L_{\text{avg}} < (n + 0.5)L_0$  and holes form when  $(n - 0.5)L_0 < L_{\text{avg}} < nL_0$ . The opposite is true for asymmetric wetting: islands form when  $(n - 0.5)L_0 < L_{\text{avg}} < nL_0$  and holes when  $nL_0 < L_{\text{avg}} < (n + 0.5)L_0$ . "Classical" islands and holes are characterized by  $1L_0$  step heights.

The thermodynamic interactions of each block at the film boundaries (*i.e.*, substrate and free surfaces) and internal interfaces govern the morphology and orientation of BCP thin films. Unfortunately, determination of the absolute energies associated with these interfaces is prone to significant error.<sup>14</sup> For example, inference of surface free energies from contact angle goniometry generally is not sufficiently predictive to quantitatively account for the delicate balance of interfacial interactions that control the spatial arrangement of domains within a thin film. In contrast, combined quantification of film thickness and surface topography provides a powerful (qualitative) technique that can accurately elucidate the preferential interactions of a BCP on a given substrate. An as-cast BCP film with a constant thickness incommensurate to both symmetric and asymmetric wetting [*e.g.*,  $(n + 0.2)L_0$ ] will form either islands or holes (but not both) upon annealing. The topography formed will only depend upon which block wets the substrate surface (assuming that a single block wets the free surface). This effect was first described by Mansky<sup>15</sup> with PS-PMMA and utilized by Peters<sup>16</sup> for the neutralization of self-assembled monolayers (SAMs). The SAM surfaces were oxidized to different extents by varying the exposure dose of X-ray radiation. The state of oxidation at which there was a switch from formation of islands to formation of holes was interpreted to be indicative of a change in which block preferentially wet the oxidized SAMs. Combinatorial studies including surface energy and BCP film thickness have confirmed the general nature of these findings.<sup>17</sup>

Formation of perpendicular domains in BCP thin films requires nonpreferential wetting of both blocks at the substrate and free surfaces. A seminal paper by Mansky *et al.*<sup>18</sup> demonstrated a universal approach to creating such "neutral" interfaces with random copolymers derived from the constituents of the BCP. For instance, certain compositions of poly(styrene-random-methyl methacrylate) are nonpreferential surfaces for PS-PMMA block copolymer. Immobilizing the neutral surfaces by cross-linking<sup>19</sup> or end-grafting<sup>20</sup> enables application of a BCP by standard spin-coating processes. Analogous strategies for achieving neutral free (top) surfaces have been significantly more challenging. Certain block copolymers such as PS-PMMA<sup>21</sup>

and poly(styrene-block-D,L-lactide) (PS-PLA)<sup>22</sup> exhibit nonpreferential interactions with a free surface at elevated temperatures, but most do not. Recently, decoupling bulk thermodynamics from thin film wetting<sup>23</sup> and top coat<sup>24</sup> strategies have emerged as effective methods for controlling top interface interactions.

Even with the wealth of cumulative information produced over the last *ca.* 50 years on BCP thin film behavior, many questions remain. Most thin film work to date has centered around neutral surface development for PS-PMMA, which has a resolution limit of *ca.* 24 nm full pitch (*i.e.*, periodicity, termed  $L_0$ ). Neutral surface effects are reported here for two high- $\chi$  BCPs that are important because they can access significantly smaller feature sizes than PS-PMMA. Partially epoxidized poly(styrene-block-isoprene) (PS-PI) di-block copolymer, referred to as PS-PEI78 (78 mol % of the repeat units in the unsaturated PI block are epoxidized), is characterized by  $L_0 = 19$  nm, and poly(4-trimethylsilylstyrene-block-D,L-lactide) (PTMSS-PLA) has  $L_0 = 14.6$  nm.

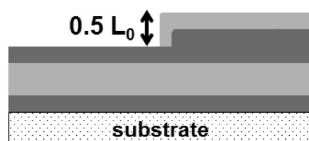
All three possible combinations of neutral interfaces have been explored with the two high- $\chi$  block copolymer thin films: (1) both the free and substrate surfaces are nonpreferential, (2) a nonpreferential free surface and a preferential substrate surface, and (3) a preferential free surface and a nonpreferential substrate surface. Neutralization of the free surface in scenarios (1) and (2) was achieved with PS-PEI78. In a recent letter,<sup>23</sup> we demonstrated that this combination of homopolymer and random copolymer blocks leads to a neutral free surface wetting condition without compromising bulk microphase separation. Scenario (3) leverages the strong preferential interaction between a single silicon-containing block and the free surface<sup>6,25</sup> using PTMSS-PLA.<sup>26</sup> The underlying substrate surfaces were designed as cross-linkable random copolymers of varying composition that enable access to different preferential PTMSS-PLA wetting, including neutral (or near neutral) conditions.

Under certain circumstances that are believed to represent a single nonpreferential interface and a single highly preferential interface, a new phenomenon was observed. Both PS-PEI78 and PTMSS-PLA exhibited  $0.5L_0$  thick islands and holes (Figure 1). This behavior is contrary to what has been previously reported and contrary to the general assumptions about "classic" thin film quantization behavior as described above. Arguments previously applied to the phase separation of bulk (three-dimensional) binary mixtures are implemented to explain the formation of these  $0.5L_0$  free surface topographies.

## RESULTS

When the partially epoxidized block copolymer PS-PEI78 is cast on a poly(styrene-random-methyl

## (a) Neutral Free Surface Preferential Substrate



## (b) Preferential Free Surface Neutral Substrate

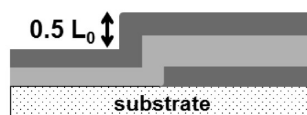


Figure 1. Schematic illustrations of  $0.5L_0$  step heights that arise with thin film lamella-forming block copolymers having one neutral and one preferential interface.

methacrylate-random-glycidyl methacrylate) mat (referred to as "SMG") and annealed, perpendicular lamellae structures form for  $L_{\text{avg}}/L_0 = 1.5, 1.9, 2.1$ , and  $2.5$  (Figure 2). This is powerful evidence for the neutrality of both the top and bottom interfaces. Only when both surfaces are neutral do BCP features orient perpendicular to the substrate independent of BCP film thickness. Importantly, the AFM data provided in Figure 2f demonstrate that the PS and PEI78 blocks can be discriminated using phase contrast mode. The free surface is thus clearly neutral for PS-PEI78 as expected based on a previous report.<sup>23</sup>

Interesting and important differences are observed between PS-PI and PS-PEI78 when annealed on a PS brush, which should be preferential to the PS block for both BCPs. PS-PI behaves as expected;<sup>27</sup> gradual variation in the average film thickness ( $L_{\text{avg}}/L_0 = 1.5, 1.7, 2.0, 2.2, 2.3$ , and  $2.5$ ) leads to a sequential change in the top-down motifs [featureless  $\rightarrow$  islands  $\rightarrow$  bicontinuous  $\rightarrow$  holes  $\rightarrow$  featureless] (Figure 3a–f) as observed by scanning electron microscopy (SEM). (Note that, in the SEMs, lighter spots are thicker and darker spots are thinner.) This is consistent with asymmetric wetting, where the PI block wets the free surface and the PS block wets the substrate (PS brush). Unexpectedly, Figure 3g–k demonstrates that the thickness dependence of the surface topology formed by PS-PEI78 differs qualitatively from the patterns produced by PS-PI. The film surfaces of the  $L_{\text{avg}} = 1.5L_0$  (Figure 3g) and  $L_{\text{avg}} = 2.0L_0$  (Figure 3i) samples are nearly featureless, while the elongated motifs exhibited by the samples with  $L_{\text{avg}} = 1.8L_0$  (Figure 3h) and  $L_{\text{avg}} = 2.3L_0$  (Figure 3k) indicate proximity to the most incommensurate film thicknesses. Atomic force micrographs (AFMs) obtained with PS-PI and PS-PEI78 ( $L_{\text{avg}} = 2.3L_0$ ) clearly indicate two significant differences between these samples. First, PS-PI generates holes with  $1L_0$  step heights as expected with classic islands and holes (Figure 4a–c), but PS-PEI78 generates unusual  $0.5L_0$  step heights (Figure 4d–f). (Note that, in the AFMs, lighter spots are thicker and darker spots are thinner.) Second, there is clear phase contrast in the AFM data for the structures generated with PS-PEI78. This indicates that there are differences in composition at the free surface and implies that both PS and PEI78 blocks are exposed, as discussed above. We assume

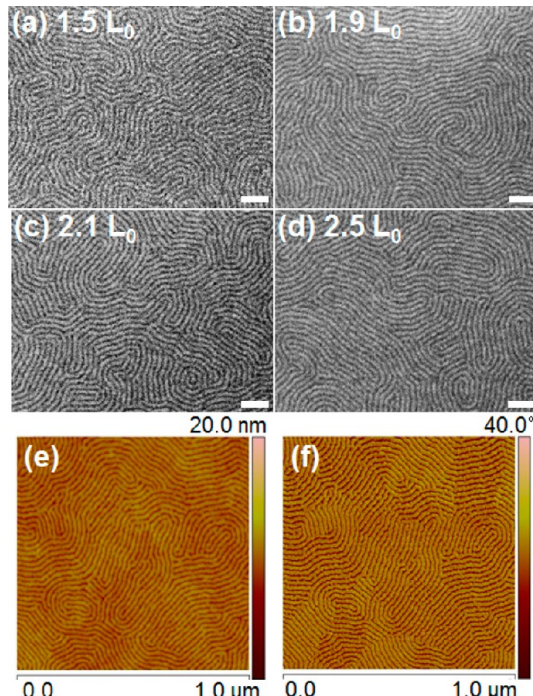


Figure 2. (a–d) Top-down SEM images of PS-PEI78 (neutral free surface) thin films with various thicknesses ( $L_{\text{avg}}/L_0 \approx 1.5, 1.9, 2.1, 2.5$ ) on SMG mat (neutral substrate surface). Scale bars correspond to 100 nm. (e,f) AFM height and phase images of PS-PEI78 on the SMG mat ( $L_{\text{avg}} \approx 2.5L_0$ ). The thin films were annealed at  $105^\circ\text{C}$  for 6 h.

that the PS brush substrate surface is PS block preferential and that these  $0.5L_0$  structures arise due to the presence of a single neutral interface, in this case the free surface. This hypothesis is further supported by the fact that reducing the BCP degree of epoxidation to 65% (done with a different symmetric PS-PI precursor diblock copolymer) leads to island and hole formation with  $1L_0$  step heights and no phase contrast between topographical features (Figure S1 in the Supporting Information).

The  $0.5L_0$  structures formed by PS-PEI78 on a PS brush are stable to extended annealing times. Figure 5 demonstrates that some lateral coarsening is observed (from  $\approx 100$ – $400$  nm to  $\approx 1$ – $3$   $\mu\text{m}$ ) consistent with  $1L_0$  step height topography,<sup>12</sup> but the quantized depth of  $0.5L_0$  holes with  $L_{\text{avg}} = 1.9$  and  $1.8L_0$  annealed for up to 12 h remains virtually unchanged. Analogously,

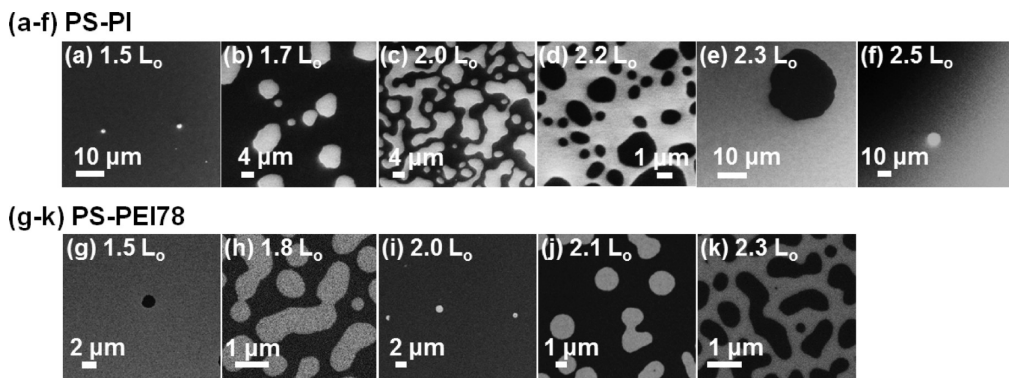


Figure 3. Top-down SEM images of thin film block copolymers with various film thicknesses on PS brushes. (a–f) PS-PI with  $L_{\text{avg}}/L_0 \approx 1.5, 1.7, 2.0, 2.2, 2.3, 2.5$ . (g–k) PS-PEI78 with  $L_{\text{avg}}/L_0 \approx 1.5, 1.8, 2.0, 2.1, 2.3$ . The thin films were annealed at 105 °C for 6–12 h.

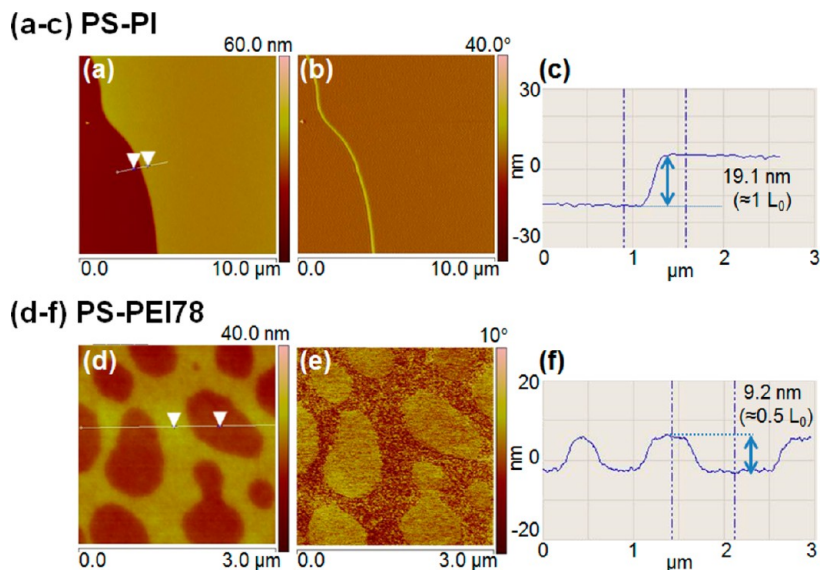


Figure 4. AFM height, phase, and height profile data of thin films ( $L_{\text{avg}} = 2.3 L_0$ ) annealed on PS brush. (a–c) PS-PI (preferential free surface) forms topography with  $1 L_0$  step heights, while (d–f) PS-PEI78 (neutral free surface) generates  $0.5 L_0$  step heights.

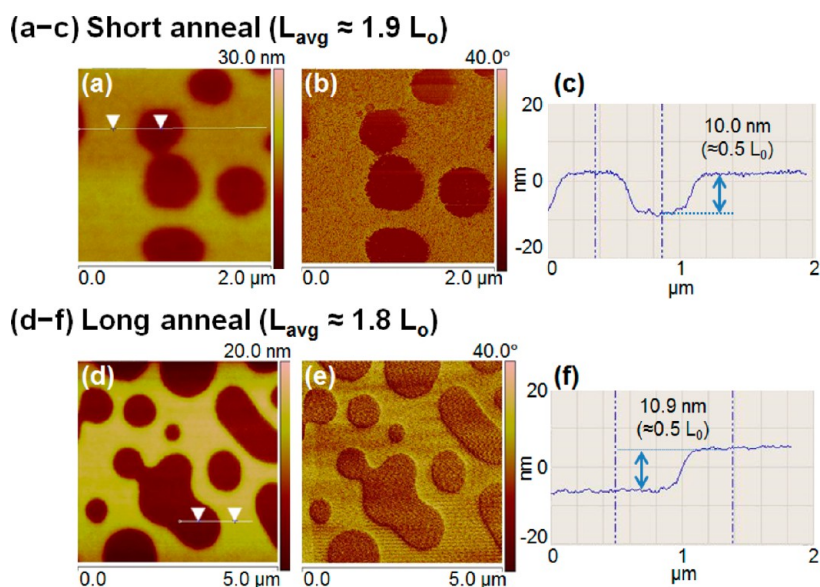


Figure 5. The  $0.5 L_0$  hole topography produced with PS-PEI78 annealed on PS brush is stable to long-term annealing as evidenced by AFM height, phase, and height profile data. (a–c) Short annealing ( $L_{\text{avg}} \approx 1.9 L_0$ ). (d–f) Long annealing (12 h,  $L_{\text{avg}} \approx 1.8 L_0$ ). Thin films were annealed at 105 °C.

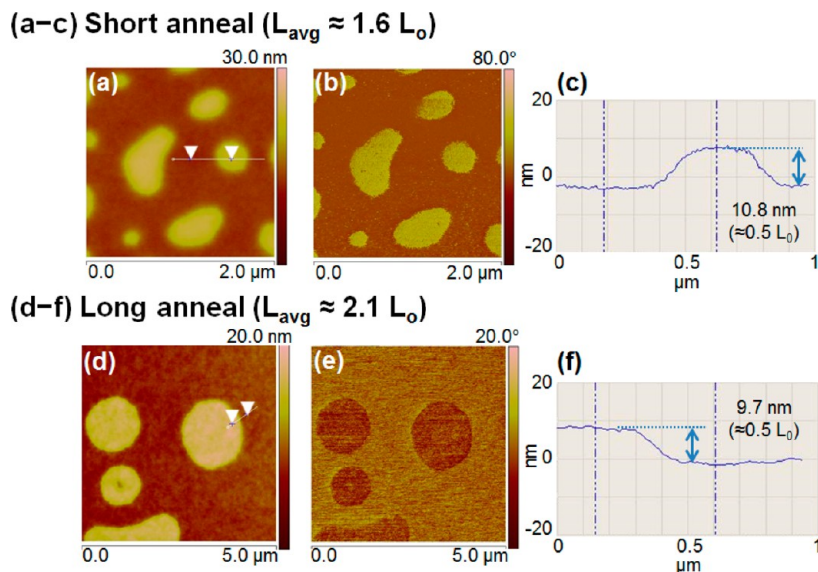


Figure 6. The  $0.5L_0$  island topography produced with PS-PEI78 annealed on PS brush is stable to long-term annealing as evidenced by AFM height, phase, and height profile data. (a–c) Short annealing ( $L_{\text{avg}} \approx 1.6L_0$ ). (d–f) Long annealing (12 h) ( $L_{\text{avg}} \approx 2.1L_0$ ). Thin films were annealed at  $105^\circ\text{C}$ .

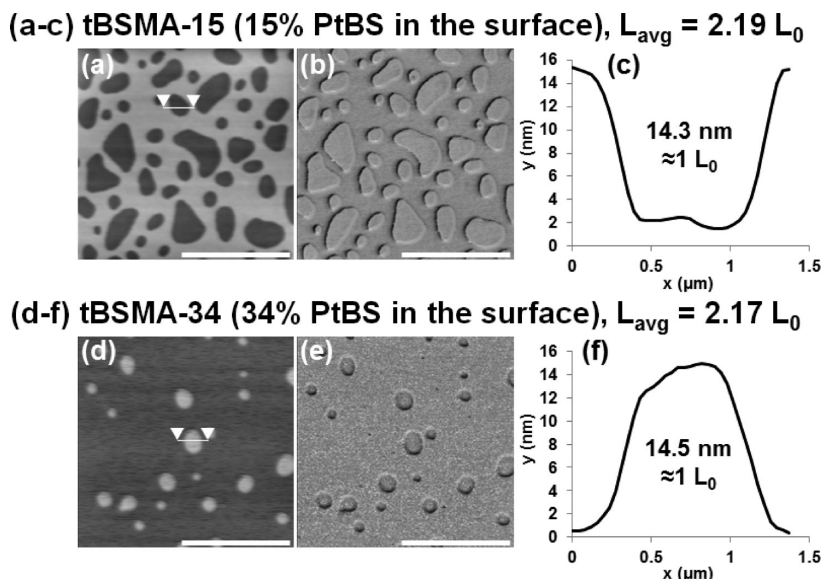


Figure 7. AFM height, phase, and height profile data of PTMSS-PLA annealed at  $150^\circ\text{C}$  for 10 min on (a–c) tBSMA-15, (d–f) tBSMA-34. Surface tBSMA-15 wets PLA, while surface tBSMA-34 wets PTMSS. Some intermediate composition(s) is (are) thus nonpreferential. The scale bars represent  $5\ \mu\text{m}$ . All height color scales span 40 nm; all phase color scales span  $15^\circ$ .

Figure 6 demonstrates that PS-PEI78  $0.5L_0$  islands are also stable to extended annealing for various film thicknesses. Step heights determined from multiple measurements on long-time annealed samples are distributed narrowly around the mean value  $0.5L_0$  with a standard deviation of less than  $0.03L_0$  ( $=0.6\text{ nm}$ ), which lies within the experimental uncertainty associated with the AFM instrument. These AFM results from PS-PEI78, reinforced by the top-down SEM data, are consistent with a parallel lamellar structure characterized by  $0.5L_0$  step heights, as depicted in Figure 1a.

PTMSS-PLA enables access to the inverse experiment. The free surface is highly preferential for the

PTMSS block,<sup>6,24</sup> but the nature of the substrate surface interactions can be changed. Cross-linkable random copolymers poly(4-*tert*-butylstyrene-*random*-methyl methacrylate-*random*-4-vinylbenzyl azide) (tBSMA) of varying composition were used to adjust the wetting behavior of PTMSS-PLA on the substrate surface, including a near neutral condition.

Figure 7 shows the results of PTMSS-PLA ( $L_{\text{avg}} \approx 2.2L_0$ ) annealed on surfaces tBSMA-15 and tBSMA-34, composed of 15 and 34 mol % of poly(4-*tert*-butylstyrene) (PtBS), respectively. Opposite topography is observed on the two surfaces; tBSMA-15 produces  $1L_0$  holes consistent with asymmetric wetting, while

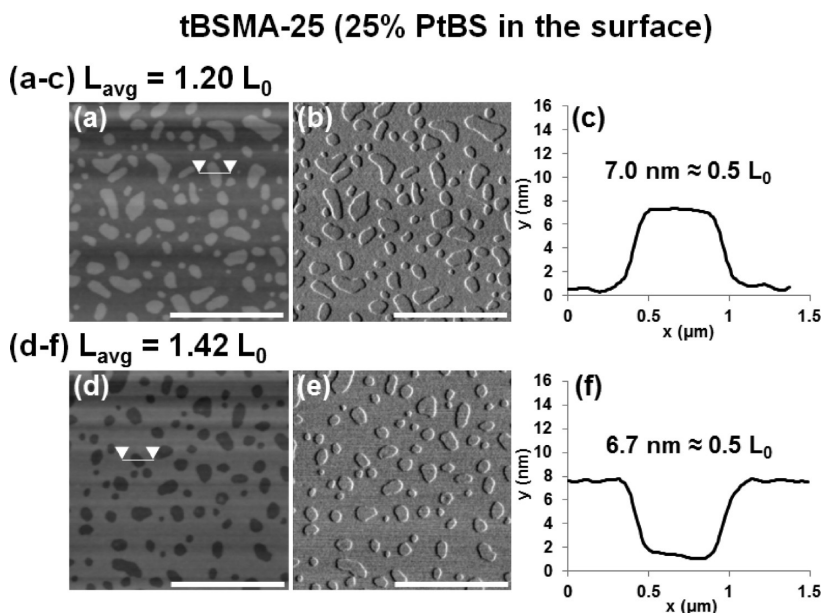


Figure 8. AFM height, phase, and height profile data of PTMSS-PLA annealed at 150 °C for 10 min on tBSMA-25 (25 mol % of PtBS content in the surface) demonstrate (a–c)  $0.5L_0$  islands and (d–f)  $0.5L_0$  holes. The scale bars represent 5  $\mu\text{m}$ . All height color scales span a 40 nm range; all phase color scales span 3°.

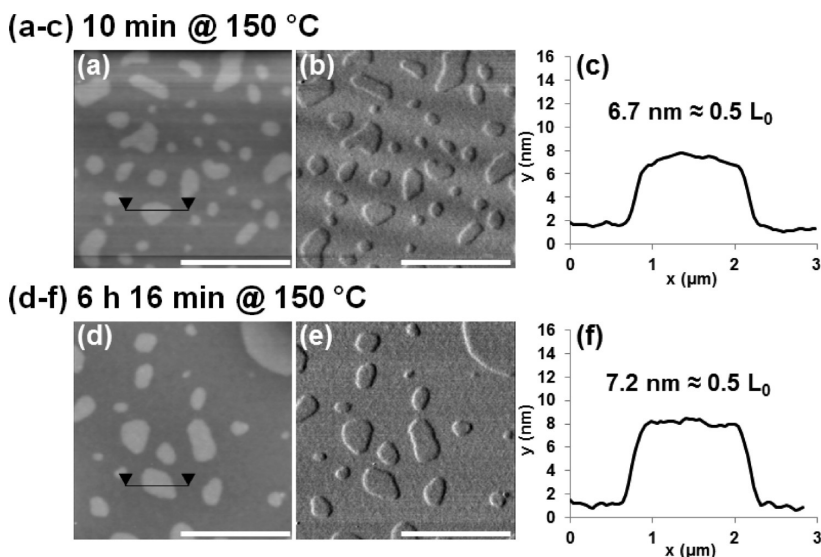


Figure 9. PTMSS-PLA  $0.5L_0$  island topography ( $L_{\text{avg}} = 1.66L_0$ ) generated on tBSMA-25 is stable to extended annealing as evidenced by AFM height, phase, and height profile data. (a–c) Annealed at 150 °C for 10 min, (d–f) annealed 150 °C for 6 h 16 min. The scale bars represent 5  $\mu\text{m}$ . All height color scales span 40 nm; all phase color scales span 3°. For clarity, note that the x-axes in (c,f) span a larger range than those in Figures 7 and 8.

tBSMA-34 produces  $1L_0$  islands consistent with symmetric wetting. Thus, the PLA block preferentially wets tBSMA-15, while the PTMSS block preferentially wets tBSMA-34. These data imply that a neutral composition for PTMSS-PLA exists between 15 and 34 mol % of PtBS. Note that uniform contrast in the AFM phase data suggests that a single block wets the free surface, consistent with the expectation that it is highly PTMSS preferential.

A mat containing 25 mol % of PtBS (tBSMA-25), a composition intermediate to tBSMA-15 and tBSMA-34, induces abnormal PTMSS-PLA thickness quantization. Figure 8 clearly shows that  $0.5L_0$  step height structures

are generated by PTMSS-PLA annealed on tBSMA-25. A sample with  $L_{\text{avg}}/L_0 = 1.20$  produces  $0.5L_0$  islands, while a sample with  $L_{\text{avg}}/L_0 = 1.42$  produces  $0.5L_0$  holes. AFM phase data are again consistent with a single block expressed at the free surface. Additionally,  $0.5L_0$  step heights form with  $L_{\text{avg}}/L_0 = 1.69$  (half islands) and  $L_{\text{avg}}/L_0 = 1.95$  (half holes) (Figure S2). Both  $0.5L_0$  island and  $0.5L_0$  hole topography generated on tBSMA-25 are stable to extended annealing times (Figures 9 and 10). Similar to PS-PEI78, some lateral coarsening is observed but the quantized height or depth of the  $0.5L_0$  structures remains virtually unchanged.

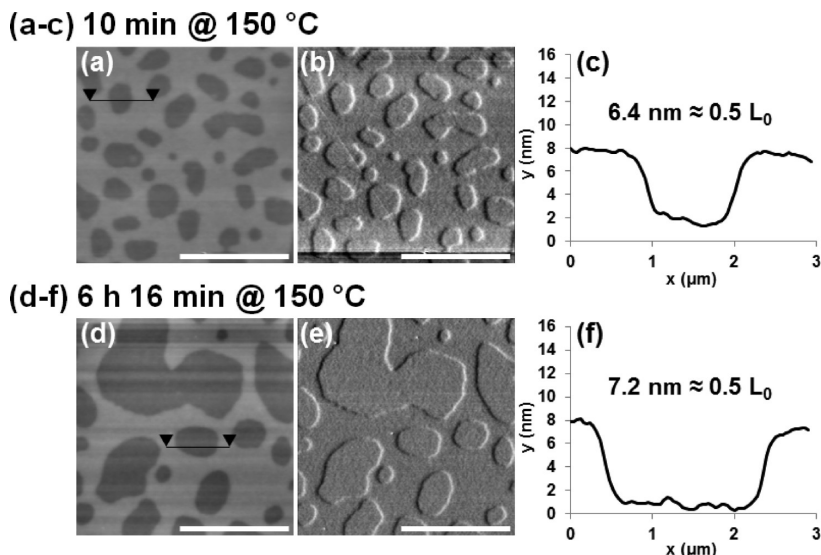


Figure 10. PTMSS-PLA  $0.5L_0$  hole topography ( $L_{avg} = 1.82L_0$ ) generated on tBSMA-25 is stable to extended annealing as evidenced by AFM height, phase, and height profile data. (a–c) Annealed at  $150\text{ }^\circ\text{C}$  for 10 min, (d–f) annealed at  $150\text{ }^\circ\text{C}$  for 6 h 16 min. The scale bars represent  $5\text{ }\mu\text{m}$ . All height color scales span 40 nm; phase color scales span  $3^\circ$ . For clarity, note that the x-axes in (c,f) span a larger range than those in Figures 7 and 8.

### PTMSS-PLA annealed on tBSMA-23

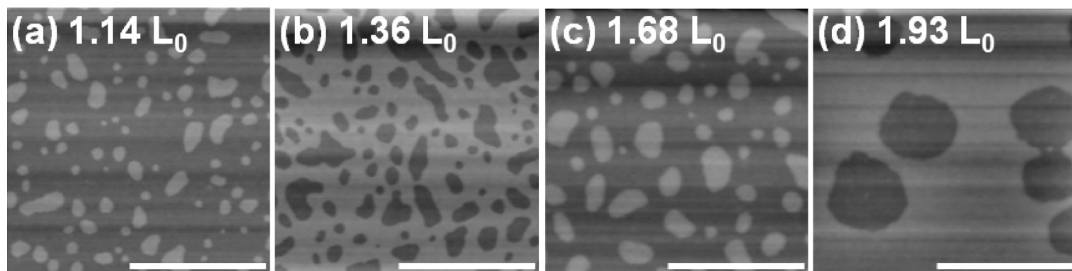


Figure 11. (a–d) Incommensurability conditions associated with  $0.5L_0$  step heights include  $(n \pm 0.25)L_0$ , i.e., half islands switch to half holes around  $L_{avg} = 1.25$  and  $1.75L_0$ . AFM height images generated with PTMSS-PLA samples annealed on tBSMA-23 at  $150\text{ }^\circ\text{C}$  for 10 min. The scale bars represent  $5\text{ }\mu\text{m}$ . All height color scales span 40 nm.

Incommensurability conditions associated with  $0.5L_0$  step height structures are distinctly different from those observed with classic  $1L_0$  islands and holes. Figure 11 shows AFM height data for four thicknesses of PTMSS-PLA annealed on tBSMA-23, all of which form  $0.5L_0$  step heights (for phase data and height profiles, see Figure S3). There is a very clear change in topography surrounding  $L_{avg} = 1.25$ ;  $L_{avg} = 1.14L_0$  forms half islands, while  $L_{avg} = 1.36L_0$  forms half holes. Both thicknesses form the same topography with classic  $1L_0$  structures. Analogously, thicknesses surrounding  $L_{avg} = 1.75L_0$  change topography;  $L_{avg} = 1.68L_0$  forms half islands, while  $L_{avg} = 1.93L_0$  forms half holes. Again, both thicknesses produce identical topography with classic  $1L_0$  structures. The  $0.5L_0$  structures generated on surface tBSMA-25 (Figures 8–10 and S2) follow the same trends. The formation of  $0.5L_0$  islands and holes appears to occur concomitant with the addition of incommensurability at  $L_{avg} = (n \pm 0.25)L_0$  (i.e.,  $1.25L_0$  and  $1.75L_0$ ). The thickness range  $nL_0 < L_{avg} < (n + 0.25)L_0$  produces half islands, while  $(n - 0.25)L_0 < L_{avg} < nL_0$

forms half holes. These conclusions are also fully consistent with the PS-PEI78 results from above (Figures 3–6).

The unexpected change in incommensurability conditions associated with the presence  $0.5L_0$  topography provides important methodology to evaluate interface neutrality. This is demonstrated with PTMSS-PLA annealed on three surfaces: tBSMA-15 (PLA preferential), tBSMA-25 (near neutral), and tBSMA-34 (PTMSS preferential). Figure 12 shows optical micrographs of two BCP thicknesses per surface,  $L_{avg} \approx 1.65L_0$  and  $L_{avg} \approx 1.85L_0$ . The change in incommensurability associated with  $0.5L_0$  structures generated on tBSMA-25 produces a change in contrast (i.e., half islands and half holes) surrounding  $L_{avg} = 1.75L_0$ , while the  $1L_0$  structures generated on tBSMA-15 and tBSMA-34 do not exhibit a change in contrast surrounding  $L_{avg} = 1.75L_0$ . This simple yet powerful experiment can be used to probe the effect of a single interface on block copolymer thin films.

In summary, topography with  $0.5L_0$  step heights always inverts surrounding  $L_{avg} = (n \pm 0.25)L_0$ . Based

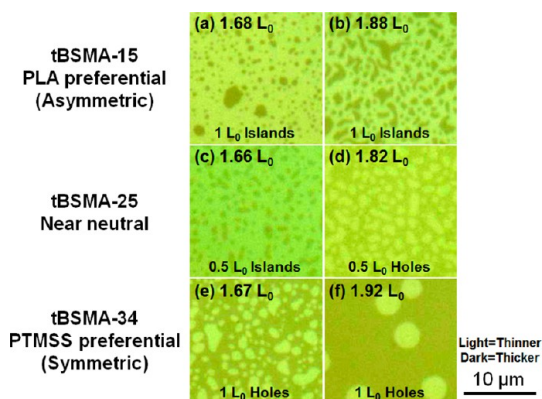


**Figure 12.** Optical microscopy can be used to screen for incommensurability associated with a single neutral interface. PTMSS-PLA annealed on tBSMA-15, 25, and 34 at 150 °C for 10 min.

on the results for both PS-PEI78 on a PS brush and PTMSS-PLA on mats with a range of compositions (e.g., tBSMA-23 and tBSMA-25), the unusual thickness dependence of  $0.5L_0$  topography appears to be uniquely associated with thin film samples confined between a nonpreferential and a preferential interface. Implications and applicability are discussed below.

## DISCUSSION

Combining appropriately designed linear homopolymer and random copolymer blocks offers unique advantages in producing thin films with remarkable morphological control. “Decoupling” the thermodynamic driving forces that govern bulk segregation and interfacial wetting through the random chemical modification of preformed polymers, such as PS-PI, provides a facile method for tuning the surface energies of block copolymers, virtually independent of microphase segregation in the bulk material.<sup>23</sup> The persistence of perpendicular ordering in thin films of PS-PEI78 when supported on the SMG mats (Figure 2), independent of the film thickness, provides incontrovertible evidence that both the free and substrate interfaces have been neutralized.<sup>28,29</sup> This indeed demonstrates that the surface energy of the PI block has changed and become comparable to that of the PS block through the partial chemical modification.

Island and hole formation with  $h = 0.5L_0$  is found for both PS-PEI78 on PS brush and PTMSS-PLA on near neutral tBSMA mats. PS-PEI78 on the PS brush produces AFM phase contrast between topographical features since the two blocks compete to wet the free surface in the layered lamellar structure. The half islands and holes observed with PTMSS-PLA are analogous to those observed with PS-PEI78. However, a lack of AFM phase contrast between PTMSS-PLA surface topography and the surrounding bulk film highlights the primary difference: a single block (PTMSS) is expressed at the free surface. Surprisingly, the unusual  $h = 0.5L_0$  finding has apparently not been described

previously in the context of a single neutral interface. Yang *et al.*<sup>30</sup> reported presumably equilibrium  $0.5L_0$  step heights generated with adjacent chemically patterned preferential surfaces that exhibited opposite wetting. This observation reinforces the internal structure proposed in the presence of a single neutral interface that can accommodate interaction with either block (Figure 1). In general, island/hole topographies are characterized by  $h = 1.0L_0$ ,<sup>13,16,31,32</sup> although several instances of metastable structures with smaller step heights ( $h < 1.0L_0$ ) have been reported at the early stage of relief formation. Examples include a broad distribution of step heights ( $h < 1.0L_0$ ) that sharpen into discrete  $h = 1.0L_0$  features upon annealing<sup>12,33</sup> and regions with  $h \approx 0.5L_0$  that appear transiently along with  $L_0$  steps.<sup>34</sup> The observed behavior reported herein with PS-PEI78 and PTMSS-PLA is qualitatively different than anecdotal examples of nonequilibrium surface motifs. PS-PEI78 (Figures 5 and 6) and PTMSS-PLA (Figures 9 and 10) both produce  $h = 0.5L_0$  features that are stable to long-term annealing and persist as the surface morphology coarsens to lateral dimensions beyond several micrometers.

The universal nature of  $h = 0.5L_0$  step heights is further established by annealing thin films of a poly(styrene-*b*-methyl methacrylate) (PS-PMMA) diblock copolymer at 230 °C, where the surface wetting tendencies of the two blocks are reported to become equivalent.<sup>21</sup> Figures S4–S9 demonstrate  $h = 0.5L_0$  islands and holes in this situation.

The observations with both PS-PEI78 on PS brush and PTMSS-PLA on tBSMA-23 and tBSMA-25 are consistent with the schematics shown in Figure 1. The illustrations highlight two possible ways that structures with step heights  $h = 0.5L_0$  can arise in thin films. In each case, a single block exclusively wets the preferential interface, but the neutral interface contacts both blocks. PS-PEI78 on PS brush facilitates the direct observation of the neutral interface since AFM is intrinsically a top surface measurement technique. AFM phase contrast demonstrates that surface topography is characterized by separate regions of contact between each block and the free surface (Figure 1a). These conclusions presumably translate to the opposite interfacial neutralization, PTMSS-PLA on tBSMA-23 and tBSMA-25, but the observation of neutral interface wetting is difficult to observe directly. Due to the strongly preferential interaction of PTMSS with the free surface, proving unequivocally that tBSMA-23 and tBSMA-25 are indeed perfectly neutral for PTMSS-PLA is challenging in lieu of additional top surface functionalization. Thickness-independent perpendicular orientation can only be achieved when the substrate materials are coupled with a neutral top surface, a topic of ongoing research that will be reported in a forthcoming publication. However, PTMSS-PLA provides confirmation that a single block wets the preferential

interface when  $0.5L_0$  topography is formed, insight that complements the data obtained with PS-PEI78 on PS brush. Coupled with the PS-PEI78 results, the generation of  $h = 0.5L_0$  topography for PTMSS-PLA only on surfaces that must be compositionally near neutral strongly implicates nonpreferential substrate interactions as the cause, as depicted in Figure 1b.

The inversion of the topographic features surrounding  $L_{\text{avg}} = (n \pm 0.25)L_0$  that arise with  $h = 0.5L_0$  provides powerful methodology that can be used to evaluate the neutrality of block copolymers and interfacial modifiers. The results for both PS-PEI78 on PS brush and PTMSS-PLA on tBSMA-23 and tBSMA-25 suggest that the formation of  $h = 0.5L_0$  features in either case is indicative of successful neutralization at a single interface. Therefore, block copolymers designed to neutralize free surface interactions can be screened on highly preferential substrate surfaces, or block copolymers with highly preferential free surface interactions can be analyzed to find nonpreferential substrates. Both possibilities were presented herein. In principle, the analysis need not even quantify the height profile for  $h = 0.5L_0$ . If there is a single neutral interface, a change in topographical features (islands and holes) will occur between a sample with thickness  $(n - 0.5)L_0 < L_{\text{avg}} < (n - 0.25)L_0$  and one  $(n - 0.25)L_0 < L_{\text{avg}} < nL_0$ , while the topography will remain unchanged if no neutral interface is present. The analysis can be performed entirely with an optical microscope (as demonstrated in Figure 12) rather than, for instance, an AFM, a cost difference measured in orders of magnitude. Even extremely small thickness differences (*ca.* 7 nm) between "half" structures and the surrounding matrix can be resolved optically.

Phase separation of initially homogeneous binary mixtures of polymers (and many other condensed systems)<sup>35,36</sup> in three dimensions (bulk) generally proceeds by two distinct kinetically controlled mechanisms: nucleation and growth (NG) and spinodal decomposition (SD).<sup>37</sup> Factors, such as the mixture composition and quench depth relative to the equilibrium (bimodal) and stability (spinodal) limits control the rate of structural evolution and the morphology of the resulting two-phase system. Symmetry breaking surfaces can modify blends that are homogeneous in the bulk state, leading to two-dimensional layered structures in the thin film limit.<sup>38,39</sup> Numerous studies conducted over the past two and a half decades have dealt with the formation of two-phase and ordered morphologies in thin layers of homopolymer blends.

The initial formation and subsequent coarsening of relief structures in thin film block copolymers bear some resemblance to the transient morphologies that develop during phase separation of unstable bulk binary mixtures. Incommensurability between the initial average film thickness  $L_{\text{avg}}$  and the natural microdomain period  $L_0$ , combined with the incompressible

nature of polymer melts, leads to the formation of terraces on the free surface, and the mechanisms that describe the transition from an initially smooth to textured interface have been studied both theoretically and experimentally.<sup>40–43</sup> The morphology of islands and holes formed through NG or SD depends on various factors, such as the thermal ramping rate<sup>44</sup> and the initial film thickness.<sup>45</sup> Shull adapted an analytical approach originally developed for the early stages of spinodal decomposition in binary mixtures in modeling the formation of hole/island motifs in thin film block copolymers.<sup>40</sup> Similar to the development of directed spinodal waves in thin film polymer blends,<sup>38,39</sup> composition waves propagate from interfaces and interfere with each other in block copolymer thin films during annealing.<sup>46,47</sup> The critical domain size required for the hole/island structures to survive the action of thermal fluctuations during the initial stage was estimated,<sup>48</sup> and a number of growth mechanisms were proposed.<sup>12,48–50</sup>

The free energy of formation associated with nuclei of heights  $h = 0.5L_0$  and  $h = 1.0L_0$  can be used to explain the formation of the relief structures obtained in the thin PS-PEI78 films. Slow thermal ramping rates ( $\approx 1$  °C/min, similar to what was used for annealing PS-PEI78) have been found to favor the NG mechanism in island/hole formation.<sup>44</sup> Achieving a critical nucleus size is the principle barrier that must be overcome for subsequent growth of the surface morphology. The free energy of a nucleus is controlled by three factors: (1) interfacial energy at the free surface, (2) elastic strain energy associated with the normalized thickness  $L_{\text{avg}}/L_0$ , and (3) line tension that results from the defects formed at the boundaries of the topographic structures. Roughening of films inherently occurs upon annealing a mixed, solvent-cast state.<sup>51,52</sup> During the formation of nonuniform variations in the film thickness, the smaller thickness gradient associated with  $h = 0.5L_0$  relative to  $h = 1.0L_0$  should favor the formation of half-step nuclei. Of course, the large difference in the surface energy between the blocks in PS-PI overwhelms any such advantage, leading to the formation of structures with  $h = 1.0L_0$ .

A transition zone separates regions of parallel lamellae (*i.e.*, islands and holes) regardless of the value of  $h$ . Experiments have shown that the free energy penalty associated with features containing a small radius of curvature causes the transition zone to broaden considerably as illustrated in Figure S10, necessitating a reconstruction of the underlying morphology.<sup>53</sup> For example, perpendicular lamellae can accommodate a continuously varying transition zone thickness but require splicing onto the parallel layers at the transition boundaries; this can be accommodated by an interfacial arrangement such as Scherk's surface.<sup>54,55</sup> Figure S11 shows the edge profiles of structures for  $h = 1.0L_0$  (PS-PI) and  $h = 0.5L_0$  (PS-PEI78) obtained using AFM

measurements. The transition width ( $\Delta x$ ) has been estimated as the difference in the lateral positions that correspond vertically to 20 and 80% of the step heights ( $\Delta x = x|_{y=0.8h} - x|_{y=0.2h}$ ). Based on the profiles in Figure S11,  $\Delta x/h$  ranges from 5–6 and 6–8 for  $h = 1.0L_0$  and  $h = 0.5L_0$ , respectively. Previous studies report significantly larger step widths for structures with  $h = 1.0L_0$ .<sup>32,54</sup> Normalized transition widths  $\Delta x/h$  for PTMSS-PLA with  $h = 1.0L_0$  (calculated from Figure 7) fall roughly in the range of 9–13. Some roundness to the peaks in the height traces makes exact calculations of  $\Delta x$  somewhat arbitrary. For  $h = 0.5L_0$ , the range of  $\Delta x/h \sim 11$ –18 is slightly larger than the range for  $h = 1.0L_0$  and all measured PS-PEI78 transition widths.

The morphology of the transition zone is expected to be established soon after the initially formed topological features begin to coarsen, analogous to the establishment of an equilibrium interfacial thickness following either nucleation or the initial stages of spinodal decomposition in phase-separating polymer blends.<sup>56,57</sup> The exact structure of the transition zone likely depends on many factors, including the exact copolymer composition, molecular weight, dispersity, statistical segment lengths, and possibly whether the free surface or substrate interface is preferentially wet. These differences could contribute to the larger transition zones measured for PTMSS-PLA compared to PS-PEI78. Intuitively, microdomain structures with negative Gauss interfacial curvature are anticipated, by analogy to the microdomain structures found adjacent to lamellae in bulk specimens, such as, gyroid and perforated lamellae<sup>58</sup> and Scherk's surface found at the boundary between orthogonally arranged lamellar grains.<sup>55</sup> Another way to relieve the local strain is to embed cylindrical domains underneath portions of the edges of island and hole structures for symmetric block copolymers.<sup>59</sup> AFM images provide evidence of such intermediate morphologies in the transition zone at the edges surrounding the island and hole structures of PS-PEI78 and PS-PMMA (Figure S9). These features are difficult to resolve and are not always visible in the AFM measurements. Alternatively, the block copolymer could partially disorder in portions of the transition zone, although this should become prohibitively expensive in free energy as the segregation strength increases. Liu *et al.*<sup>59</sup> documented reconstructed island edges for large molecular weight ( $M_n > 100$  kg/mol) but not low molecular weight ( $M_n < 40$  kg/mol) poly(styrene-*b*-2-vinylpyridine) (PS-PVP) block copolymers. The absence of well-described microphase segregation in highly constrained block copolymer systems also has been reported.<sup>9,47</sup>

The relief structures with  $h = 0.5L_0$ , which initially form as a result of surface neutralization, may face energetic barriers in transforming into structures with  $h = 1.0L_0$ . Such a transformation would involve a transport of polymers that already constitute well-built

structures with large domains (~micrometers) (Figures 5, 6, 9, and 10). The possibility of “pinning” should not be dismissed in explaining the observation of  $0.5L_0$  step heights even after 12 h of annealing PS-PEI78 or >6 h of annealing PTMSS-PLA. The persistence of the intermediate morphologies, or pinning of stages, due to kinetic traps that prevent the system from reaching the thermodynamic equilibrium has been commonly observed in various systems that go through phase separations. Examples include development of microstructures in metal alloys, spinodal decomposition of off-critical polymer blends,<sup>60</sup> coarsening of phase-separated polymer blends in thin films,<sup>61</sup> path-dependent morphologies in micelles<sup>62</sup> or ternary mixtures of oil/water/block copolymer surfactant,<sup>63</sup> the formation of spherical morphologies of bulk block copolymers with solvent annealing,<sup>64</sup> and the growth of hole/island structures in thin film block copolymers that form parallel lamellae.<sup>65,66</sup> Sometimes, the specific kinetically frozen states are sought after for their desirable properties, such as perpendicular domain orientations in the case of solvent annealing block copolymer thin films.<sup>67</sup> Various mechanisms have been suggested to be responsible for such pinning, including surface curvature elasticity,<sup>27</sup> loss of interfacial continuity when a percolating morphology breaks up into clusters,<sup>60</sup> glassy cores,<sup>68</sup> or the incompatibility between cores and solvents<sup>62</sup> that suppress chain exchange in micelles. All these examples display kinetic barriers that must be overcome before reaching true thermodynamic equilibrium. Similarly, the local transformation of structures from  $h = 0.5L_0$  into  $h = 1.0L_0$  would be inhibited by unfavorable diffusion normal to the microdomain interfaces<sup>69,70</sup> and suppressed by the requirement for long-range lateral transport of material.

## CONCLUSIONS

A study of block copolymer thin films with three combinations of interfaces at least one of which is nonpreferential is reported. Unusual topographical step heights with half the bulk periodicity ( $0.5L_0$ ) were generated when a block copolymer was confined between a neutral and a preferential interface. PS-PEI78 (neutral free interface) exhibits such behavior when supported on a preferential PS brush. Both constituents of the block copolymer were exposed to the free surface as demonstrated by AFM phase data. In contrast, PTMSS-PLA has a strongly preferential free surface and produces  $0.5L_0$  step heights only when supported on a neutral (or very near neutral) substrate. AFM phase contrast measurements demonstrate that PTMSS-PLA exposes a single block to the free surface. Incommensurate film thicknesses associated with  $0.5L_0$  step heights were found to include  $L_{\text{avg}} = (n \pm 0.25)L_0$ , distinctly different than simple asymmetric ( $nL_0$ ) and

symmetric  $[(n - 0.5)L_0]$  wetting. The observation of  $0.5L_0$  step heights therefore provides a simple, powerful, and

accurate method for determining the surface neutrality of a single interface.

## METHODS

**Material Synthesis and Bulk Characterization.** *PS-PI and PS-PEI78.* A poly(styrene-*b*-isoprene) (PS-PI) diblock copolymer was synthesized using anionic polymerization, followed by controlled epoxidation of the PI block using dimethyl dioxirane (DMD),<sup>23</sup> resulting in a diblock copolymer referred to as PS-PEI78. Size exclusion chromatography (SEC) (Waters 717 Autosampler with Waters 2410 Refractive Index Detector; Viscotek VE2001 with 302-050 Tetra Detector Array; THF mobile phase) was used to determine the number average molecular weight ( $M_n = 21.3$  kg/mol) and polydispersity index (PDI = 1.06) of PS-PI. The composition  $f_1 = 0.51$  (volume fraction of PI) of the PS-PI diblock and the extent of epoxidation in PS-PEI78 (78 mol %) were determined using proton nuclear magnetic resonance ( $^1\text{H}$  NMR) (VAC-300 Autosampler, IBM Instruments). Differential scanning calorimetry (Q1000 DSC, TA Instruments) was utilized (heating rate of  $\pm 10$  °C/min) to determine the glass transition temperatures ( $T_g$ ) of the polymer. The order-disorder transition temperature ( $T_{ODT}$ ) of the PS-PI was identified by dynamic mechanical spectroscopy (Ares 2, Rheometrics) based on the steep drop in the linear dynamic elastic shear modulus ( $G'$ ) obtained while heating at 1 °C/min. Small-angle X-ray scattering (SAXS) experiments (Argonne National Laboratory) were performed on bulk specimens at room temperature after annealing in vacuum at 105 °C for 3–6 h. The one-dimensional form of the scattering intensity,  $I(q)$  ( $q = 4\pi\lambda^{-1}\sin(\theta/2)$  is the scattering wavevector), was obtained by reducing the data recorded on a two-dimensional area detector.

**PTMSS-PLA.** 4-Trimethylstylene monomer and symmetric poly(4-trimethylsilylstyrene-*b*-D,L-lactide) were prepared as reported previously.<sup>26</sup>

Table 1 shows molecular characterization results for the three block copolymers utilized herein. Nearly symmetric PS-PI and PS-PEI78 ( $f_{PS} = 0.49$ ) and PTMSS-PLA ( $f_{PTMSS} = 0.50$ ) diblock copolymers were prepared for this study. Full bulk characterization data are reported in the Supporting Information (Figures S12–S17). SEC traces of PS-PI, PS-PEI78, and thermally annealed PS-PEI78 are shown in Figure S12. Annealing PS-PEI78 at 105 °C for 6 h does not produce discernible degradation of the

material. However, annealing at higher temperatures (e.g.,  $> 160$  °C) for 6 h led to the presence of some amount of swollen gel when the polymer was immersed in THF, suggestive of thermal cross-linking through the epoxides.<sup>71,72</sup> For this reason,  $T_{ODT}$  is undetermined for PS-PEI78;  $T_{ODT} = 182$  °C for PS-PI. Two distinct glass transitions are evident in the DSC traces for PS-PI and PS-PEI78 (Figure S13);  $T_{g-PS} \approx 82$  °C and  $T_{g-PI} \approx -62$  °C for PS-PI and  $T_{g-PS} \approx 78$  °C and  $T_{g-PEI78} \approx 3$  °C for PS-PEI78. An increase in the glass transition temperature of the rubbery block with chemical modification is expected based on previous reports dealing with epoxidized natural rubbers.<sup>73</sup> Diffraction peaks evident in the SAXS patterns (Figure S14) are consistent with lamellar morphologies for bulk PS-PI and PS-PEI78, as expected based on the symmetric compositions of these block copolymers. The bulk periodicities ( $L_0$ ) of PS-PI and PS-PEI78 estimated from the primary peak positions of the SAXS patterns are 18.9 and 19.1 nm, respectively. A substantial decrease in the scattered intensity associated with PS-PEI78 relative to PS-PI is attributed to the near electron density matching created by the presence of oxygen in the epoxidized compound.<sup>23</sup> PTMSS-PLA SEC traces (Figure S15) are consistent with complete and monodisperse block growth. SAXS data on a sample annealed at 160 °C (Figure S16) verify a lamellar morphology with  $L_0 \approx 14.6$  nm. DSC traces (Figure S17) are consistent with two glass transition temperatures ( $T_{g-PTMSS} = 104$  °C,  $T_{g-PLA} = 49$  °C) similar to those previously reported for PTMSS-PLA of similar molecular weight.<sup>26</sup>

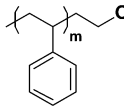
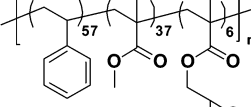
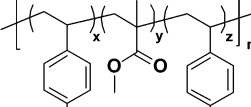
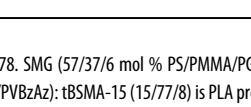
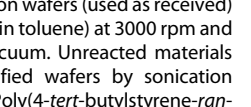
**Mat/Brush Preparation.** Random copolymers (28.5 kg/mol, PDI = 1.50) containing styrene ( $m_S = 0.57$ ), methyl methacrylate ( $m_{MMA} = 0.37$ ), and cross-linkable functional groups (glycidyl methacrylate) ( $m_{GMA} = 0.06$ ) were synthesized using nitroxide-mediated living free radical polymerization (NMP),<sup>74</sup> where  $m$  represents the mole fraction. The mat (denoted SMG) was spin-coated from a solution (0.2–0.5 wt % in toluene) at 3000 rpm and subsequently cross-linked at 160–190 °C for 24 h under vacuum. Hydroxyl-terminated poly(styrene) homopolymers (PS-OH, 3.7 and 6.0 kg/mol) were purchased from Polymer Source, Inc. (sample nos. P7499-SOH, P7590-SOH) and used as brush materials without any further purification. The polymer

**TABLE 1. Characterization Data of the Three Diblock Copolymers Utilized in the Present Study<sup>a</sup>**

Block Polymers	Structure	$M_n$ (kg/mol)	$\mathfrak{D}$	$f_{PS}$ or $f_{PTMSS}$	$T_g$ (°C)	$T_{ODT}$
PS-PI		21.3	1.06	0.49	82, -62	182
PS-PEI78		23.1	1.09	0.49	78, 3	N/A
PTMSS-PLA		12.1	1.06	0.50	104, 48	N/A

<sup>a</sup> PS-PI (preferential free surface), PS-PEI78 (nonpreferential free surface), and PTMSS-PLA (preferential free surface).

**TABLE 2. Characterization Data of the Substrate Surfaces Utilized in the Present Study<sup>a</sup>**

Substrate Surface Treatments	Structure	M <sub>n</sub> (kg/mol)	D	Substrate Surface Interaction
PS-OH		3.7, 6.0	1.06	PS Preferential
SMG		28.5	1.50	Neutral for PS-PEI78
tBSMA-15		31.6	1.38	PLA Preferential
tBSMA-23, 25		38.5, 35.9	1.70, 1.66	Near Neutral for PTMSS-PLA
tBSMA-34		34.2	1.44	PTMSS Preferential

<sup>a</sup> PS-OH is PS preferential for PS-PI and PS-PEI78. SMG (57/37/6 mol % PS/PMMA/PG) is PS preferential for PS-PI and neutral for PS-PEI78. tBSMA surfaces were used with PTMSS-PLA. Compositions (mol % PtBS/PMMA/PVBzAz): tBSMA-15 (15/77/8) is PLA preferential; tBSMA-23 (23/71/6) and tBSMA-25 (25/69/6) are near neutral; tBSMA-34 (34/59/7) is PTMSS preferential.

brushes were grafted onto bare silicon wafers (used as received) by spin-coating a solution (1.0 wt % in toluene) at 3000 rpm and annealing at 190 °C for 24 h in vacuum. Unreacted materials were removed from the PS-modified wafers by sonication (3×, 5 min each) with toluene. Poly(4-*tert*-butylstyrene-*ran*-methyl methacrylate-*ran*-4-vinylbenzyl azide) surfaces were prepared by conventional free radical copolymerization in a two-step process analogous to previous reports.<sup>75,76</sup> The materials are denoted tBSMA-yy, where yy refers to the mol % of the poly(4-*tert*-butylstyrene) component (i.e., tBSMA-15, tBSMA-23, tBSMA-25, and tBSMA-34) (Table 2). 4-*tert*-Butylstyrene, methyl methacrylate, and 4-vinylbenzyl chloride were copolymerized to low conversion (<10% mass recovery) to minimize monomer drift. The two principal components, poly(4-*tert*-butylstyrene) and poly(methyl methacrylate), were selected due to their large interaction parameter.<sup>77</sup> Upon isolation, the copolymers were postpolymerization functionalized with sodium azide. Low quantities (ca. 6–8 mol %) of poly(4-vinylbenzyl azide) were included for cross-linking. Cross-linkable substrate surface treatments were dissolved as 0.5 wt % solutions in toluene and spin-coated at 3500 rpm to afford uniform films with ca. 15 nm thickness. Films were cross-linked at 250 °C for 5 min on a hot plate in air, cooled to room temperature, and washed three times with toluene at 3500 rpm. Final film thicknesses were measured five times and averaged, with typical values ca. 14 nm, an average range of 0.1 nm and an average standard deviation of 0.04 nm.

**Surface Treatment Characterization.** Table 2 shows the chemical structures and characterization data of the substrate surfaces utilized to produce different substrate wetting conditions for the three block copolymers. SEC data (Figure S18) of the four poly(4-*tert*-butylstyrene-*ran*-methyl methacrylate-*ran*-4-vinylbenzyl azide) surfaces (tBSMA, referred to by the mol % PtBS content) are consistent with monomodal molecular weight distributions.

**PS-PI Thin Film Preparation and Characterization.** Uniform thin films were obtained by spin-coating solutions of PS-PEI78 (1.0–1.5 wt %, in toluene) on cross-linked SMG mats and PS brushes. Average film thicknesses ranging from 1.5L<sub>0</sub> to 2.6L<sub>0</sub> (L<sub>0</sub> = 2π/q<sub>1</sub>, where q<sub>1</sub> is the principle Bragg reflection measured by SAXS) were determined by ellipsometry (AutoEL-II, Rudolph

Research). The spin-coated thin films were first placed in an oven chamber under vacuum (<10 mTorr), then N<sub>2</sub> gas was constantly flowed into the chamber so that the pressure within the chamber remained at ≈1.0 Torr throughout the thermal annealing process. The oven chamber was heated at the rate of 1.0 °C/min to the set temperature and cooled slowly (<0.25 °C/min) to room temperature once the heater was turned off. The annealing temperatures reported in this paper were read from a thermocouple attached to a bare Si wafer, which was placed in the chamber during thermal annealing. The annealing time refers to the period that the sample temperature was maintained at 105 °C, excluding the time required for ramping up and down. The expression “short-time annealing” referred to herein corresponds to a thermal annealing procedure in which the heater is turned off as soon as the temperature of the annealing chamber reaches 105 °C.

Thin films of PS-PI, PS-PEI78, and PS-PMMA were characterized by scanning electron microscopy (SEM) (LEO 1550-VP FESEM) and atomic force microscopy (AFM) (Nanoscope III Multimode AFM, Digital Instruments) (Materials Science Center, Univ. of Wisconsin—Madison). AFM was utilized in tapping mode, with tips of resonant frequencies in the range of 170–310 kHz, to measure the height profiles and the phase images of the BCP thin films. The largest scanned area in AFM was restricted to ≈11 × 11 μm<sup>2</sup> due to the availability of headers with recent calibrations, and samples of a known topography were measured to check the calibrations. AFM phase images are generally sensitive to near surface properties, such as adhesion, viscoelasticity, and hardness, and the phase contrast often permits discrimination of the domain type at the top surface.<sup>78</sup> The difference in glass transition temperatures between PS and epoxidized PI (PEI) blocks (Figure S13) was anticipated to enhance the phase contrast at the measurement condition (room temperature) since the PS block is glassy and the PEI block is rubbery.<sup>79</sup> While the topography extracted from AFM height profiles was quantitatively reproducible, the phase contrast showed some variability but nonetheless allowed discrimination of the surface characteristics.

**PTMSS-PLA Thin Film Preparation and Characterization.** A Brewer CEE 100CB spincoater was used to coat thin films of PTMSS-PLA onto tBSMA mats. Film thicknesses were

characterized by ellipsometry (J.A. Woollam Co, Inc. VB 400 VASE ellipsometer) with a 65° angle of incidence and wavelengths from 382 to 984 nm. Uniform PTMSS-PLA films were applied from variable solution concentrations (0.5–1.2 wt %) in toluene at various spin speeds. Block copolymer film thicknesses were measured five times and averaged, with an average range of 0.3 nm and an average standard deviation of 0.1 nm. Samples were annealed on a hot plate (Heraeus Vacutherm Type VT 6060 P from Kendro) and quickly cooled to room temperature on a metal block. Optical micrographs were collected with an Olympus BX60 at 100× magnification. Tapping mode atomic force microscopy was performed with an Asylum MFP-3D utilizing tips with resonant frequencies of 170–310 kHz. Combustion analysis performed by Midwest Microlab LLC was used to calculate the relative compositions of the substrate surface treatments tBSMA-15, 23, 25, and 34.

**Conflict of Interest:** The authors declare no competing financial interest.

**Acknowledgment.** Financial support for this work was provided by the National Science Foundation—Nanoscale Science and Engineering Center at the University of Wisconsin—Madison (Grant No. DMR-0832760). The authors thank Chris Thode for providing the cross-linkable brush material (SMG). This material is partially based upon work supported by the National Science Foundation Scalable Nanomanufacturing Program under Grant No. 1120823, Nissan Chemical Company, and the Rashid Engineering Regents Chair. C.J.E. thanks the Welch Foundation (Grant No. F-1709) for partial financial support.

**Supporting Information Available:** Top-down SEM and AFM images of poly(styrene-*b*-isoprene) diblock copolymers (12.3–10.5 kg/mol) with partial epoxidation of 65%. AFM data for PTMSS-PLA annealed on various substrate surfaces. Top-down SEM and AFM images of poly(styrene-*b*-methyl methacrylate) diblock copolymers (PS-PMMA, 66–63.5 kg/mol, Polymer Source, Inc.) above SMG cross-linkable mat and PS brush. Schematic illustrations of thin film morphologies. Block copolymer and surface treatment characterization data. This material is available free of charge via the Internet at <http://pubs.acs.org>.

## REFERENCES AND NOTES

- Hillmyer, M. A. Nanoporous Materials from Block Copolymer Precursors. *Adv. Polym. Sci.* **2005**, *190*, 137–181.
- Xin-Yu, B.; He, Y.; Bencher, C.; Li-Wen, C.; Huixiang, D.; Yongmei, C.; Chen, P. T. J.; Wong, H. S. P. In *SRAM, NAND, DRAM Contact Hole Patterning Using Block Copolymer Directed Self-Assembly Guided by Small Topographical Templates*; 2011 IEEE International Electron Devices Meeting (IEDM), 5–7 Dec. 2011; 2011; pp 7.7.1–7.7.4.
- Ruiz, R.; Kang, H.; Detchevry, F. A.; Dobisz, E.; Kercher, D. S.; Albrecht, T. R.; de Pablo, J. J.; Nealey, P. F. Density Multiplication and Improved Lithography by Directed Block Copolymer Assembly. *Science* **2008**, *321*, 936–939.
- Bradford, E. B.; Vanzo, E. Ordered Structures of Styrene-Butadiene Block Copolymers in the Solid State. *J. Polym. Sci., Part A: Polym. Chem.* **1968**, *6*, 1661–1670.
- Vanzo, E. Ordered Structures of Styrene-Butadiene Block Copolymers. *J. Polym. Sci., Part A: Polym. Chem.* **1966**, *4*, 1727–1730.
- Clark, D. T.; Peeling, J.; O’Malley, J. M. Application of ESCA to Polymer Chemistry. VIII. Surface Structures of AB Block Copolymers of Polydimethylsiloxane and Polystyrene. *J. Polym. Sci.: Polym. Chem. Ed.* **1976**, *14*, 543–551.
- Green, P. F.; Christensen, T. M.; Russell, T. P.; Jerome, R. Surface Interaction in Solvent-Cast Polystyrene-Poly(methyl methacrylate) Diblock Copolymers. *Macromolecules* **1989**, *22*, 2189–2194.
- Thomas, H. R.; O’Malley, J. J. Surface Studies on Multi-component Polymer Systems by X-ray Photoelectron Spectroscopy. Polystyrene/Poly(ethylene oxide) Diblock Copolymers. *Macromolecules* **1979**, *12*, 323–329.
- Henkee, C. S.; Thomas, E. L.; Fetters, L. J. The Effect of Surface Constraints on the Ordering of Block Copolymer Domains. *J. Mater. Sci.* **1988**, *23*, 1685–1694.
- Coulon, G.; Russell, T. P.; Deline, V. R.; Green, P. F. Surface-Induced Orientation of Symmetric, Diblock Copolymers: A Secondary Ion Mass-Spectrometry Study. *Macromolecules* **1989**, *22*, 2581–2589.
- Russell, T. P.; Coulon, G.; Deline, V. R.; Miller, D. C. Characteristics of the Surface-Induced Orientation for Symmetric Diblock PS/PMMA Copolymers. *Macromolecules* **1989**, *22*, 4600–4606.
- Coulon, G.; Collin, B.; Ausserre, D.; Chatenay, D.; Russell, T. P. Islands and Holes on the Free Surface of Thin Diblock Copolymer Films. I. Characteristics of Formation and Growth. *J. Phys. (Paris)* **1990**, *51*, 2801–2811.
- Coulon, G.; Ausserre, D.; Russell, T. P. Interference Microscopy on Thin Diblock Copolymer Films. *J. Phys. (Paris)* **1990**, *51*, 777–786.
- Strobel, M.; Lyons, C. S. An Essay on Contact Angle Measurements. *Plasma Processes Polym.* **2011**, *8*, 8–13.
- Mansky, P.; Russell, T. P.; Hawker, C. J.; Pitsikalis, M.; Mays, J. Ordered Diblock Copolymer Films on Random Copolymer Brushes. *Macromolecules* **1997**, *30*, 6810–6813.
- Peters, R. D.; Yang, X. M.; Kim, T. K.; Sohn, B. H.; Nealey, P. F. Using Self-Assembled Monolayers Exposed to X-rays To Control the Wetting Behavior of Thin Films of Diblock Copolymers. *Langmuir* **2000**, *16*, 4625–4631.
- Smith, A. P.; Sehgal, A.; Douglas, J. F.; Karim, A.; Amis, E. J. Combinatorial Mapping of Surface Energy Effects on Diblock Copolymer Thin Film Ordering. *Macromol. Rapid Commun.* **2003**, *24*, 131–135.
- Mansky, P.; Liu, Y.; Huang, E.; Russell, T. P.; Hawker, C. Controlling Polymer–Surface Interactions with Random Copolymer Brushes. *Science* **1997**, *275*, 1458–1460.
- Ryu, D. Y.; Shin, K.; Drockenmuller, E.; Hawker, C. J.; Russell, T. P. A Generalized Approach to the Modification of Solid Surfaces. *Science* **2005**, *308*, 236–239.
- Huang, E.; Rockford, L.; Tussell, T. P.; Hawker, C. J. Nano-domain Control in Copolymer Thin Films. *Nature* **1998**, *395*, 757–758.
- Mansky, P.; Russell, T. P.; Hawker, C. J.; Mays, J.; Cook, D. C.; Satija, S. K. Interfacial Segregation in Disordered Block Copolymers: Effect of Tunable Surface Potentials. *Phys. Rev. Lett.* **1997**, *79*, 237–240.
- Keen, I.; Yu, A.; Cheng, H.-H.; Jack, K. S.; Nicholson, T. M.; Whittaker, A. K.; Blakey, I. Control of the Orientation of Symmetric Poly(Styrene)-block-Poly(*D,L*-Lactide) Block Copolymers Using Statistical Copolymers of Dissimilar Composition. *Langmuir* **2012**, *28*, 15876–15888.
- Kim, S.; Nealey, P. F.; Bates, F. S. Decoupling Bulk Thermodynamics and Wetting Characteristics of Block Copolymer Thin Films. *ACS Macro Lett.* **2012**, *1*, 11–14.
- Bates, C. M.; Seshimo, T.; Maher, M. J.; Durand, W. J.; Cushen, J. D.; Dean, L. M.; Blachut, G.; Ellison, C. J.; Willson, C. G. Polarity-Switching Top Coats Enable Orientation of Sub-10-nm Block Copolymer Domains. *Science* **2012**, *338*, 775–779.
- Jung, Y. S.; Ross, C. A. Orientation-Controlled Self-Assembled Nanolithography Using a Polystyrene-Polydimethylsiloxane Block Copolymer. *Nano Lett.* **2007**, *7*, 2046–2050.
- Cushen, J. D.; Bates, C. M.; Rausch, E. L.; Dean, L. M.; Zhou, S. X.; Willson, C. G.; Ellison, C. J. Thin Film Self-Assembly of Poly(trimethylsilylstyrene-*b*-*D,L*-Lactide) with Sub-10 nm Domains. *Macromolecules* **2012**, *45*, 8722–8728.
- Smith, A. P.; Douglas, J. F.; Meredith, J. C.; Amis, E. J.; Karim, A. Combinatorial Study of Surface Pattern Formation in Thin Block Copolymer Films. *Phys. Rev. Lett.* **2001**, *87*, 015503/1–015503/4.
- Han, E.; Kang, H.; Liu, C.-C.; Nealey, P. F.; Gopalan, P. Graphoepitaxial Assembly of Symmetric Block Copolymers on Weakly Preferential Substrates. *Adv. Mater.* **2010**, *22*, 4325–4329.
- Pickett, G. T.; Balazs, A. C. Equilibrium Orientation of Confined Diblock Copolymer Films. *Macromolecules* **1997**, *30*, 3097–3103.

30. Yang, X. M.; Peters, R. D.; Nealey, P. F.; Solak, H. H.; Cerrina, F. Guided Self-Assembly of Symmetric Diblock Copolymer Films on Chemically Nanopatterned Substrates. *Macromolecules* **2000**, *33*, 9575–9582.

31. Coulon, G.; Russell, T. P.; Deline, V. R.; Green, P. F. Surface-Induced Orientation of Symmetric, Diblock Copolymers: A Secondary Ion Mass-Spectrometry Study. *Macromolecules* **1989**, *22*, 2581–2589.

32. Maaloum, M.; Ausserre, D.; Chatenay, D.; Coulon, G.; Gallot, Y. Edge Profile of Relief 2D Domains at the Free Surface of Smectic Copolymer Thin Films. *Phys. Rev. Lett.* **1992**, *68*, 1575–1578.

33. Joly, S.; Raquois, A.; Paris, F.; Hamdoun, B.; Auvray, L.; Ausserre, D. Early Stage of Spinodal Decomposition in 2D. *Phys. Rev. Lett.* **1996**, *77*, 4394–4397.

34. Maaloum, M.; Ausserre, D.; Chatenay, D.; Gallot, Y. Spinodal-Decomposition-like Patterns via Metastable State Relaxation. *Phys. Rev. Lett.* **1993**, *70*, 2577–2580.

35. Cahn, J. W. Spinodal Decomposition. *Trans. Metall. Soc. AIME* **1968**, *242*, 166–180.

36. Huang, J. S.; Goldberg, W. I.; Bjerkaas, A. W. Phase Separation in a Critical Binary Liquid Mixture. Spinodal Decomposition. *Phys. Rev. Lett.* **1974**, *32*, 921–923.

37. Hashimoto, T.; Kumaki, J.; Kawai, H. Time-Resolved Light-Scattering-Studies on Kinetics of Phase-Separation and Phase Dissolution of Polymer Blends. 1. Kinetics of Phase-Separation of a Binary Mixture of Polystyrene and Poly(vinyl methyl-ether). *Macromolecules* **1983**, *16*, 641–648.

38. Jones, R. A. L.; Norton, L. J.; Kramer, E. J.; Bates, F. S.; Wiltzius, P. Surface-Directed Spinodal Decomposition. *Phys. Rev. Lett.* **1991**, *66*, 1326–1329.

39. Krausch, G.; Dai, C.-A.; Kramer, E. J.; Bates, F. S. Spinodal Decomposition in Thin Polymer Films. *Ber. Bunsen-Ges.* **1994**, *98*, 446–448.

40. Shull, K. R. Mean-Field Theory of Block Copolymers: Bulk Melts, Surfaces, and Thin-Films. *Macromolecules* **1992**, *25*, 2122–2133.

41. Walton, D. G.; Kellogg, G. J.; Mayes, A. M.; Lambooy, P.; Russell, T. P. A Free-Energy Model for Confined Diblock Copolymers. *Macromolecules* **1994**, *27*, 6225–6228.

42. Koneripalli, N.; Singh, N.; Levicky, R.; Bates, F. S.; Gallagher, P. D.; Satija, S. K. Confined Block-Copolymer Thin-Films. *Macromolecules* **1995**, *28*, 2897–2904.

43. Lambooy, P.; Russell, T. P.; Kellogg, G. J.; Mayers, A. M.; Gallagher, P. D.; Satija, S. K. Observed Frustration in Confined Block Copolymers. *Phys. Rev. Lett.* **1994**, *72*, 2899–2902.

44. Singh, N.; Kudrle, A.; Sikka, M.; Bates, F. S. Surface Topography of Symmetric and Asymmetric Polyolefin Block Copolymer Films. *J. Phys. II* **1995**, *5*, 377–396.

45. Vignaud, G.; Gibaud, A.; Grubel, G.; Joly, S.; Ausserre, D.; Legrand, J. F.; Gallot, Y. Ordering of Diblock PS-PBMA Thin Films: An X-ray Reflectivity Study. *Physica B* **1998**, *248*, 250–257.

46. Fredrickson, G. H. Surface Ordering Phenomena in Block Copolymer Melts. *Macromolecules* **1987**, *20*, 2535–2542.

47. Russell, T. P.; Coulon, G.; Deline, V. R.; Miller, D. C. Characteristics of the Surface-Induced Orientation for Symmetric Diblock PS/PMMA Copolymers. *Macromolecules* **1989**, *22*, 4600–4606.

48. Grim, P. C. M.; Nyrkova, I. A.; Semenov, A. N.; ten Brinke, G.; Hadzioannou, G. The Free-Surface of Thin Diblock Copolymer Films: Experimental and Theoretical Investigations on the Formation and Growth of Surface-Relief Structures. *Macromolecules* **1995**, *28*, 7501–7513.

49. Bassereau, P.; Brodbeck, D.; Russell, T. P.; Brown, H. R.; Shull, K. R. Topological Coarsening of Symmetric Diblock Copolymer Films: Model 2D Systems. *Phys. Rev. Lett.* **1993**, *71*, 1716–1719.

50. Ausserre, D.; Chatenay, D.; Coulon, G.; Collin, B. Growth of Two-Dimensional Domains in Copolymer Thin Films. *J. Phys. (Paris)* **1990**, *51*, 2571–2580.

51. Mayes, A. M.; Russell, T. P.; Bassereau, P.; Baker, S. M.; Smith, G. S. Evolution of Order in Thin Block-Copolymer Films. *Macromolecules* **1994**, *27*, 749–755.

52. Collin, B.; Chatenay, D.; Coulon, G.; Ausserre, D.; Gallot, Y. Ordering of Copolymer Thin-Films As Revealed by Atomic Force Microscopy. *Macromolecules* **1992**, *25*, 1621–1622.

53. Turner, M. S.; Maaloum, M.; Ausserre, D.; Joanny, J. F.; Kunz, M. Edge Dislocations in Copolymer Lamellar Films. *J. Phys. II* **1994**, *4*, 689–702.

54. Carvalho, B. L.; Thomas, E. L. Morphology of Steps in Terraced Block Copolymer Films. *Phys. Rev. Lett.* **1994**, *73*, 3321–3324.

55. Gido, S. P.; Gunther, J.; Thomas, E. L.; Hoffman, D. Lamellar Diblock Copolymer Grain-Boundary Morphology. 1. Twist Boundary Characterization. *Macromolecules* **1993**, *26*, 4506–4520.

56. Bates, F. S.; Wiltzius, P. Spinodal Decomposition of a Symmetric Critical Mixture of Deuterated and Protonated Polymer. *J. Chem. Phys.* **1989**, *91*, 3258–3274.

57. Hashimoto, T.; Takenaka, M.; Jinnai, H. Scattering Studies of Self-Assembling Processes of Polymer Blends in Spinodal Decomposition. *J. Appl. Crystallogr.* **1991**, *24*, 457–466.

58. Khandpur, A. K.; Forster, S.; Bates, F. S.; Hamley, I. W.; Ryan, A. J.; Bras, W.; Almdal, K.; Mortensen, K. Polyisoprene-Polystyrene Diblock Copolymer Phase Diagram near the Order-Disorder Transition. *Macromolecules* **1995**, *28*, 8796–8806.

59. Liu, Y.; Rafailovich, M. H.; Sokolov, J.; Schwarz, S. A.; Bahal, S. Effects of Surface Tension on the Dislocation Structures of Diblock Copolymers. *Macromolecules* **1996**, *29*, 899–906.

60. Hashimoto, T.; Takenaka, M.; Izumitani, T. Spontaneous Pinning of Domain Growth during Spinodal Decomposition of Off-Critical Polymer Mixtures. *J. Chem. Phys.* **1992**, *97*, 679–689.

61. Sung, L.; Karim, A.; Douglas, J. F.; Han, C. C. Dimensional Crossover in the Phase Separation Kinetics of Thin Polymer Blend Films. *Phys. Rev. Lett.* **1996**, *76*, 4368–4371.

62. Jain, S.; Bates, F. S. Consequences of Nonergodicity in Aqueous Binary PEO-PB Micellar Dispersions. *Macromolecules* **2004**, *37*, 1511–1523.

63. Lee, S.; Arunagirinathan, M. A.; Bates, F. S. Path-Dependent Morphologies in Oil/Water/Diblock Copolymer Mixtures. *Langmuir* **2010**, *26*, 1707–1715.

64. Shibayama, M.; Hashimoto, T.; Kawai, H. Ordered Structure in Block Polymer-Solutions. 5. Equilibrium and Non-equilibrium Aspects of Microdomain Formation. *Macromolecules* **1983**, *16*, 1434–1443.

65. Smith, A. P.; Douglas, J. F.; Meredith, J. C.; Amis, E. J.; Karim, A. High-Throughput Characterization of Pattern Formation in Symmetric Diblock Copolymer Films. *J. Polym. Sci., Part B: Polym. Phys.* **2001**, *39*, 2141–2158.

66. Coulon, G.; Collin, B.; Chatenay, D.; Gallot, Y. Kinetics of Growth of Islands and Holes on the Free Surface of Thin Diblock Copolymer Films. *J. Phys. II* **1993**, *3*, 697–717.

67. Sinturel, C.; Vayer, M.; Morris, M.; Hillmyer, M. A. Solvent Vapor Annealing of Block Polymer Thin Films. *Macromolecules* **2013**, *46*, 5399–5415.

68. Zhang, L. F.; Eisenberg, A. Multiple Morphologies of Crew-Cut Aggregates of Polystyrene-*b*-Poly(acrylic acid) Block-Copolymers. *Science* **1995**, *268*, 1728–1731.

69. Dalvi, M. C.; Lodge, T. P. Parallel and Perpendicular Chain Diffusion in a Lamellar Block Copolymer. *Macromolecules* **1993**, *26*, 859–861.

70. Hamersky, M. W.; Tirrell, M.; Lodge, T. P. Anisotropy of Diffusion in a Lamellar Styrene-Isoprene Block Copolymer. *Langmuir* **1998**, *14*, 6974–6979.

71. Poh, B. T.; Tan, B. K. Mooney Scorch Time of Epoxidized Natural Rubber. *J. Appl. Polym. Sci.* **1991**, *42*, 1407–1416.

72. Gelling, I. R. Modification of Natural Rubber Latex with Peracetic Acid. *Rubber Chem. Technol.* **1985**, *58*, 86–96.

73. Gnecco, S.; Pooley, A.; Krause, M. Epoxidation of Low-Molecular Weight *Euphorbia lacticula* Natural Rubber with *In Situ* Formed Performic Acid. *Polym. Bull.* **1996**, *37*, 609–615.

74. Han, E.; Stuen, K. O.; La, Y. H.; Nealey, P. F.; Gopalan, P. Effect of Composition of Substrate-Modifying Random Copolymers on the Orientation of Symmetric and Asymmetric

Diblock Copolymer Domains. *Macromolecules* **2008**, *41*, 9090–9097.

75. Bang, J.; Bae, J.; Lowenhielm, P.; Spiessberger, C.; Given-Beck, S. A.; Russell, T. P.; Hawker, C. J. Facile Routes to Patterned Surface Neutralization Layers for Block Copolymer Lithography. *Adv. Mater.* **2007**, *19*, 4552–4557.

76. Bates, C. M.; Strahan, J. R.; Santos, L. J.; Mueller, B. K.; Bamgbade, B. O.; Lee, J. A.; Katzenstein, J. M.; Ellison, C. J.; Willson, C. G. Polymeric Cross-Linked Surface Treatments for Controlling Block Copolymer Orientation in Thin Films. *Langmuir* **2011**, *27*, 2000–2006.

77. Kennemur, J. G.; Hillmyer, M. A.; Bates, F. S. Synthesis, Thermodynamics, and Dynamics of Poly(4-*tert*-butylstyrene-*b*-methyl methacrylate). *Macromolecules* **2012**, *45*, 7228–7236.

78. Rehse, N.; Knoll, A.; Magerle, R.; Krausch, G. Surface Reconstructions of Lamellar ABC Triblock Copolymer Mesostuctures. *Macromolecules* **2003**, *36*, 3261–3271.

79. Fasolka, M. J.; Mayes, A. M.; Magonov, S. N. Thermal Enhancement of AFM Phase Contrast for Imaging Diblock Copolymer Thin Film Morphology. *Ultramicroscopy* **2001**, *90*, 21–31.